Effect of S Arrangement on Fe(110) Properties at 1/3 Monolayer Coverage: A DFT Study

Michelle J. S. Spencer, Ian K. Snook, and Irene Yarovsky*

Applied Physics, RMIT University, GPO Box 2476V, Victoria, 3001, Australia

Received: August 23, 2005; In Final Form: November 10, 2005

Using density functional theory calculations, we compare the relative stabilities and properties of different arrangements of S on Fe(110) at a 1/3 monolayer coverage, including two observed experimentally. For all studied arrangements, S is adsorbed in the three high-symmetry adsorption sites: 4-fold hollow, 3-fold hollow, bridge, and atop sites. The binding energy, work function change, adsorption geometry, charge density distribution, magnetic properties, and density of states are determined and compared. The most stable overlayer arrangement corresponds to the overlayer seen by experiment after dissociative adsorption of H_2S and has S adsorbed in 4-fold hollow sites. In the other arrangements, the S atoms are located closer to each other on the surface reducing the stability of the overlayer. S causes a minor adsorbate-induced reconstruction of the Fe surface and quenches the magnetic moment of the Fe atoms it bonds to directly. It adsorbs as an electropositive species, causing a positive work function change and forms polar covalent bonds to the surface.

1. Introduction

Sulfur (S) contamination of iron (Fe) has important implications in many industrial processes, and the effect it has on the metal's surface properties is a major factor in current and future applications of the metal. Previous studies have shown that as the S coverage increases, different overlayer arrangements form on the Fe(110) surface (ref 1 and refs therein). At coverages corresponding to 1/3 monolayer (ML), however, there is more than one overlayer arrangement observed experimentally.

Kelemen et al.[2] found that an overlayer, described as $c(3 \times 1)$, was formed following the appearance of a $p(2 \times 2)$ arrangement after H_2S adsorption at 150 °C on Fe(110). They also observed the same overlayer after segregation of S from the bulk via heating, but found that it did not afford the same degree of control over the S surface concentration as after H_2S adsorption. Oudar[3] also observed a $c(3 \times 1)$ structure and suggested that the S adsorbs in sites where the coordination of the substrate atoms is maximized. Berbil-Bautista et al.[4] also recently showed that this arrangement forms after H_2S adsorption and dissociation on three-dimensional Fe islands on W(110). This overlayer arrangement is illustrated in Figure 1 and is referred to as overlayer A.

In contrast to the above studies, Weissenrieder et al.[5] found an overlayer, described as $p(3 \times 1)$, formed after annealing an Fe(110) single crystal to 700 °C to yield a S coverage corresponding to 1/3 ML. Taga et al.[6] also found this overlayer formed after annealing an Fe(111) surface to 600 °C. As the temperature was raised, (110) facets developed on the surface, and the S concentration increased, resulting in a surface reconstruction and facet structure described as Fe(110)$p(3 \times 1)$-S. This overlayer arrangement is shown in Figure 1 and is referred to as overlayer B.

To investigate these different overlayers formed at 1/3 ML coverage on Fe(110), and to complement our previous studies of how S coverage affects the surface properties of Fe(110),[1,7] we performed density functional theory (DFT) calculations of the two overlayer arrangements described above, as well as an alternative arrangement, referred to as overlayer C and illustrated in Figure 1, where the S atoms are arranged in rows along the $[\bar{1}11]$ direction. We determine the most stable surface arrangement and relate the findings to the observed experimental overlayers. For each of the three overlayer arrangements, S was adsorbed in four different high-symmetry adsorption sites (atop, bridge, 3-fold hollow, and 4-fold hollow). A range of surface properties, including the structure, work function values, vibrational frequencies, charge density arrangement, magnetic properties, and density of states are also presented.

2. Method

2.1 Computational Details. All calculations were performed using the plane wave pseudopotential Vienna ab initio simulation package (VASP),[8−10] which performs fully self-consistent DFT calculations to solve the Kohn−Sham equations.[11] The generalized gradient spin approximation, using the functional of Perdew and Wang (PW91),[12] was employed. The plane wave cutoff energy was 308.76 eV. Core electrons were replaced by ultrasoft pseudopotentials.[13] K-space sampling was performed using the scheme of Monkhorst and Pack,[14] with a mesh of $6 \times 6 \times 1$, shown previously[7] to be sufficient for this sized supercell. Our previous work showed this approach to give a good description of bulk, surface, and interfacial properties of Fe,[15−18] FeS_2,[19−21] as well as S/Fe(110) systems.[1,7,22,23] For the calculation of fractional occupancies, a broadening approach by Methfessel and Paxton[24] was used with order $N = 1$ and smearing width 0.1 eV for the Fe(110) and S/Fe(110) slabs. The isolated S atom was modeled in a $15 \times 15 \times 15$ Å cell using a Gaussian broadening method, a smearing width of 0.1, and a cutoff energy equal to that used for Fe. For accurate calculation of total energies and magnetic moment values, the tetrahedron scheme[25] was employed. A Weigner−Seitz radius of 1.3 and 1.164 Å was employed for Fe and S, respectively.

2.2. Surface Models. The Fe surfaces were modeled using the supercell approach, where periodic boundary conditions are applied to the central supercell so that it is reproduced

* Corresponding author. E-mail: irene.yarovsky@rmit.edu.au. Telephone: +61 3 9925 2571. Fax: +61 3 9925 5290.

10.1021/jp054769f CCC: $33.50
Published on Web 12/22/2005

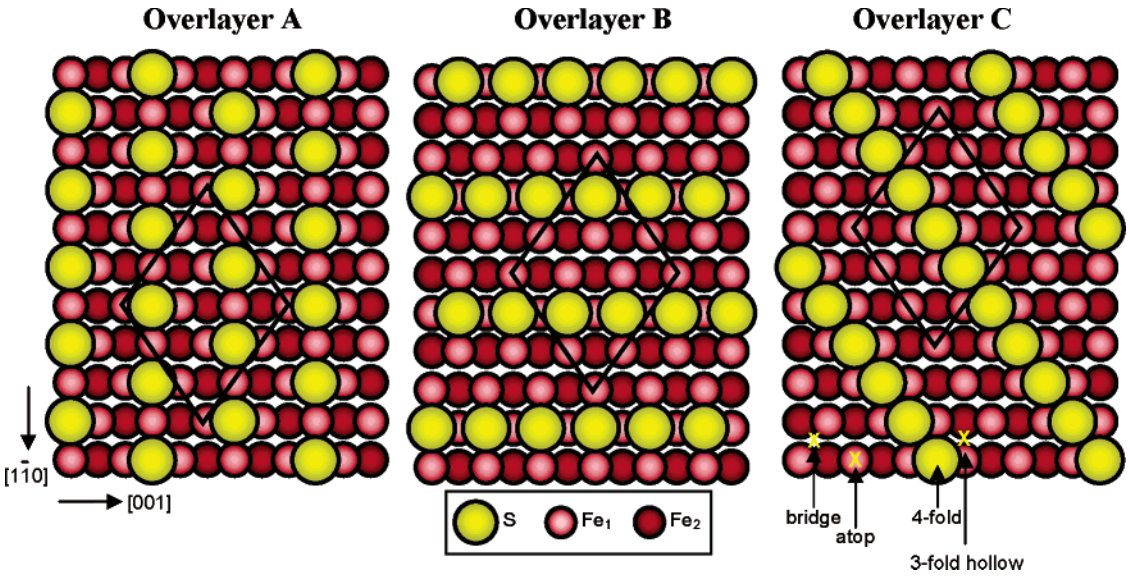

Figure 1. Top view of the Fe(110) surface showing different surface arrangements of S atoms corresponding to 1/3 ML coverage, with the corresponding unit cells used to model the arrangements. S was adsorbed in atop, bridge, 3-fold, and 4-fold hollow sites (only the 4-fold hollow site is shown).

periodically throughout space. Surfaces corresponding to the (110) Miller plane were cleaved from a crystal structure of (bcc) Fe,. For each surface arrangement, a 3×3 cell was used with three adsorbed S atoms (Figure 1). The cells comprised five Fe layers, and the S atoms were adsorbed on one side of the surface slab only in atop, bridge, 3-fold hollow, or 4-fold hollow sites. The surface was produced by replication of the central supercell in the *x*,*y* directions. A vacuum spacer of ~10 Å was inserted in the *z* direction. A lattice constant value of 2.855 Å was used, as this is the lattice constant obtained by bulk cell optimization using the same computational parameters.[7] Calculations were performed allowing the S and top three Fe layers to relax while keeping the bottom two Fe layers fixed at the bulk geometry.

The S binding energy (BE) per atom was calculated using the following equation:

$$\mathrm{BE} = [E_{\mathrm{slab+3S}} - 3E_{\mathrm{S}} - \mathrm{E}_{\mathrm{slab}}]/3$$

where $E_{\mathrm{slab+3S}}$ is the total energy of the relaxed S/Fe(110) system with three adsorbed S atoms, E_{slab} is the total energy of the relaxed clean Fe(110) slab and E_{S} is the total energy of an isolated S atom. Hence, a more negative binding energy indicates a more favorable structure. To determine the type of stationary point found by the geometry optimization, vibrational frequency calculations were performed by diagonalizing a finite difference construction of the Hessian matrix with displacements of 0.04 Å (allowing only the S atoms to move).

For the calculated work function values, a dipole correction (as implemented in VASP[26,27]) was added in the direction perpendicular to the surface (as we have an asymmetric slab with the adsorbate placed on only one side of the slab). Calculations of the electrostatic potential within the vacuum region of each supercell then showed a clear distinction between the vacuum level of each side of the slab. The work function values, Φ, were then calculated using the follwing equation:

$$\Phi = E_{\mathrm{vac}} - E_{\mathrm{F}}$$

where E_{vac} is the electrostatic potential in the vacuum region of the supercell on the adsorbate side and E_{F} is the energy of the Fermi level.

3. Results and Discussion

3.1. Binding Energy and Work Function Measurements. The calculated binding energy (BE) values for S adsorbed in atop, bridge, 3-fold hollow, and 4-fold hollow sites in the three different surface arrangements are shown in Table 1, along with the classification of the stationary points found. The 3-fold hollow site was found to be a stationary point only for overlayer C. For overlayers A and B, the S atoms moved into the 4-fold hollow sites during the geometry optimization, indicating that the 3-fold hollow site is not a stationary point for these overlayer arrangements.

The most stable structure was found to be the overlayer A arrangement with S adsorbed in 4-fold hollow sites. This site is also the only minimum for this arrangement, with the bridge and atop sites being higher-order saddle points.

For overlayer B, the 4-fold hollow site was again the favored site, but neither this site nor the other sites considered were found to be minima. The binding energies were all less than the values for the overlayer A arrangements in the respective sites, indicating that this arrangement is less favored.

For overlayer C, the 4-fold hollow site was found to have the same binding energy as the 3-fold hollow site but, unlike overlayer A, was found to be a transition state with the 3-fold hollow site being a minimum. The binding energy of these structures, however, was lower than either of the 4-fold hollow overlayer A and B arrangements. Again, the atop and bridge sites were found to be higher order stationary points.

These findings are in agreement with the previous experimental studies, where the least stable overlayer C, determined from our calculations, is the overlayer that has not been observed experimentally. The fact that we did not find a minimum structure for the overlayer B arrangement, which corresponds to that seen after S segregation,[5] suggests that the presence of S in the underlying substrate may stabilize this structure. For overlayer A, the experimental studies do not appear to have identified the S adsorption site, but the findings are in agreement with Oudar,[3] who suggested that the S adsorbs in the sites where the coordination of the substrate atoms is maximized.

It is interesting to note that the binding energy value of the 4-fold hollow overlayer A arrangement is greater than any of the values calculated previously for S adsorbed on Fe(110) at

TABLE 1: Calculated Properties of S/Fe(110) in Different Arrangements at 1/3 ML Coverage[a]

overlayer arrangement	adsorption site	BE (eV)	type of SP	$\Delta\phi$ (eV)	d(S−Fe) (Å)	$d_\perp$(S−Fe_1) (Å)	magnitude of relaxation (Å) δz_1	δz_2	δz_3
overlayer A[2,4]	atop	−4.75	hos	0.71	2.07	1.78/9	**−0.07**	0.07	0.03
							0.21	0.05	0.02
	bridge	−5.43	hos	0.41	2.16	1.55	**−0.01**	0.04	0.02
							0.18	0.02	
	4-fold hollow	−6.00	0	0.36	2.19	1.39[b]	**−0.01**	0.05	0.03
							0.20	0.04	
overlayer B[5]	atop	−4.14	hos	0.45	2.07	1.95	**−0.01**	0.07	0.03
							0.12	0.01	0.01
	bridge	−4.70	hos	0.28	2.19	1.77	**0.06**	0.04	0.02
							0.02	0.03	0.01
	4-fold hollow	−5.22	2	0.13	2.17	1.54	**0.03**	0.09	0.04
							0.13	0.03	0.03
overlayer C	atop	−3.97	hos	0.36	2.13	2.08	**0.03**	0.06	0.02
							0.90	0.04	
	bridge	−4.28	hos	0.07	2.18	1.70	**−0.01**	0.07	0.03
							0.09	0.04	0.02
								0.03	
	3-fold hollow	−4.71	0	0.02	2.25	1.66	**0.04**	0.05	0.02
							0.06	0.04	
							0.03	0.03	
								0.02	
	4-fold hollow	−4.71	1	0.00	2.26	1.66	**0.08**	0.07	0.04
							0.06	0.05	0.03

[a] Binding energy (BE); type of stationary point (SP): 0 = minimum, 1 = transition state, 2 = 2nd order saddle point, hos = higher order saddle point; change in work function value ($\Delta\phi$); shortest S−Fe distance, d(S−Fe), see Figure 1; perpendicular height of S above the top surface Fe layer, $d_\perp$(S−Fe_1); magnitude of Fe surface relaxation for top three layers. A negative value indicates a contraction of the layer toward the bulk, while a positive value indicates an expansion. Relaxation of the Fe atoms (in layer 1) that are closest to the adsorbed S are indicated in bold. [b] Corresponds to h_1 in Figure 2.

other coverages,[1] indicating it is the most stable arrangement. The next most strongly bound arrangement has S adsorbed in 4-fold hollow sites in a $p(2 \times 2)$ arrangement corresponding to 1/4 ML. These two structures correspond to the experimentally observed arrangements.

The calculated work function values, Φ, (Table 1) for all the overlayer structures examined were found to be greater than that of the clean surface, leading to positive work function changes, ΔΦ (see Table 1) and suggesting the presence of a negatively charged surface species. This is consistent with previous changes determined for 1/4 and 1/2 ML of S adsorbed on the same surface,[1] indicating a transfer of charge from the substrate to the adsorbate. The magnitude of the work function change is smaller for the more stable structures, indicating a smaller transfer of charge, leading to stabilization of the overlayer.

3.2. Surface Geometry. 3.2.1. Adsorbate-Induced Relaxation and Reconstruction. For the most stable arrangement examined (4-fold hollow overlayer A arrangement), S was found to cause a minor reconstruction as well as relaxation of the Fe(110) surface. Figure 2 shows the relaxed geometry of this overlayer, with the associated distances presented in Tables 1 and 2.

For the adsorbate-induced reconstruction, the Fe atoms most closely bound to the S were found to move so as to increase the S−Fe distance, while the next most closely bound Fe atoms did not move. Overall, this led to an increase in the S coordination. There do not appear to have been any structural parameters reported for the experimentally observed 1/3 ML coverage arrangement for comparison. However, a minor surface reconstruction was also seen for the other experimentally observed $p(2 \times 2)$ arrangement (1/4 ML coverage),[28] which was also found for the DFT modeled overlayer.[7]

For most of the other overlayer arrangements, S also caused minor surface reconstructions, with the movements again leading to an increase in the S coordination.

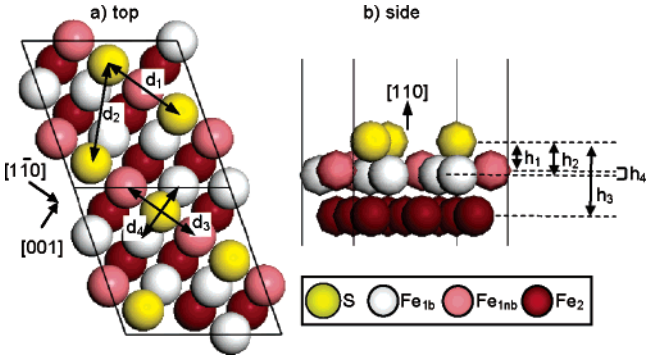

Figure 2. (a) Top and (b) side view of relaxed S/Fe(110) with S adsorbed in 4-fold hollow sites in overlayer A arrangement. Distances labeled d_n and h_n are shown in Table 2. b = bonded, nb = nonbonded.

TABLE 2: Calculated Structural Parameters for Clean Bulk-Cleaved Fe(110) and S/Fe(110) with S Adsorbed in 4-fold Hollow Sites in Overlayer A Arrangement

view	distance (Å)		clean Fe(110)	S/Fe(110)
top	d_1	(S−S)		4.04
	d_2	(S−S)		4.73
	d_3	(Fe−Fe)	4.038	4.038
	d_4	(Fe−Fe)	2.855	2.978
side	h_1	(S−Fe_{1nb})		1.39
	h_2	(S−Fe_{1b})		1.60
	h_3	(S−Fe_2)		3.57
	h_4	(Fe_{1b}−Fe_{1nb})	0.00	0.21

The adsorbed S caused relaxation of the Fe(110) surface layer atoms. The clean Fe(110) surface is essentially bulk cleaved,[18] hence the values presented in Tables 1 and 2 are determined relative to the bulk-cleaved surface values. It is interesting to note that the S causes a buckling of the top Fe layers, with atoms within the same layer relaxing by different amounts.

For the 4-fold hollow overlayer A arrangement (Figure 2), the surface relaxations were larger for the 1st and 2nd layers, and only minor for the 3rd layer, consistent with a decreasing strength of interaction between the adsorbed S and the surface as the bulk is approached. Also, surface buckling was present for the 1st and 2nd layers but not for the 3rd layer. For the 1st layer, the Fe atoms most closely bound to the adsorbed S only relaxed by 0.01 Å, but those next most closely bound relaxed by 0.2 Å. Such movements resulted in increasing the coordination of the bound S. The atoms again relaxed away from the bulk in the 2nd layer, but the movements were smaller, consistent with a weaker interaction with the adsorbed S.

Similar buckling of the 1st and 2nd Fe layers was also seen previously for some other coverages of S/Fe(110).[1,7] Again, there do not appear to be any experimental values for comparison with the 1/3 ML coverage structure.

For the other 1/3 ML arrangements, a similar trend was observed, with surface buckling also seen for the 1st and 2nd layers. Buckling of atoms in the 3rd layer was also sometimes present, but was not as pronounced as for the top layers. In general, all relaxations were positive, indicating that S causes the Fe layers to relax away from the bulk. Again, the overall trend is to increase the coordination of the adsorbed S.

3.2.2. S−Fe Bonding Distances. The shortest adsorbate−substrate bond distances, d(S−Fe), and the height of the adsorbate atom above the surface, $d_\perp$(S−Fe), were calculated for each surface arrangement (see Table 1). Due to surface buckling, the topmost Fe layer boundary is determined as the highest point on the surface. These values are indicated in Figure 2 for the 4-fold hollow overlayer A arrangement.

For each overlayer arrangement, the height of the S atom above the topmost Fe layer was found to be related to the binding energy, with the distance being smaller for the higher binding energy adsorption sites. In particular, the S was found to sit closest to the surface for the most stable 4-fold hollow overlayer A arrangement. In addition, the perpendicular S−Fe_1 distances can be related to the distances between adjacent S atoms on the surface, which are 4.038, 2.856, and 2.472 Å, for overlayers A, B, and C, respectively. Hence when the S atoms are closer together on the surface, they sit higher above the topmost Fe layer, resulting in a less stable arrangement due to adjacent S−S interactions. Hence, the more stable overlayer exists when the S atoms are separated the furthest on the surface, corresponding to overlayer A arrangement.

The shortest S−Fe distances were found to vary less than the perpendicular S−Fe distances, only differing by 0.19 Å. The distances were, however, found to increase with increasing coordination number, being generally shortest for the atop site and longest for the 4-fold hollow site, consistent with the findings for other S coverages.[1]

3.3. Magnetic Properties. Table 3 shows the calculated magnetic moment enhancements, $\Delta\mu_B$, resolved to individual Fe atoms for the most stable structures examined. They are calculated with reference to the bulk value of bcc Fe, $2.4\mu_B$, that was determined previously using the same computational parameters.[29] The $\Delta\mu_B$ values of the top layer Fe atoms that are directly bonded to the S atom (as indicated by the surface geometry) are shown in bold type in Table 3.

For all overlayers, the magnetic moment of the adsorbed S was found to be almost zero, indicating spin pairing due to bond formation between the adsorbed S and Fe surface atoms.

According to the supercell setup for all overlayers examined, the 4th and 5th Fe layers correspond to the top two layers of a clean bulk-cleaved Fe(110) surface. We previously determined that the $\Delta\mu_B$ values for the 1st, 2nd, and 3rd layers of the bulk-cleaved Fe(110) surface were 0.34, 0.12, and 0.08 μ_B, respectively.[29] As the values for the S/Fe(110) structures are almost identical to the equivalent layers on the clean surface, this suggests that there is very little or no interaction between the adsorbed S and these layers. For the 3rd Fe layer, there is a small difference in the calculated $\Delta\mu_B$ values compared to the clean surface, indicating the interaction with the adsorbed S is only weak. In contrast, larger changes are found for the 1st and 2nd layers, indicating the S interacts primarily with these layers.

TABLE 3: Calculated Magnetic Moment Enhancement Values, $\Delta\mu_B$, Resolved by Layer and Atom for S Adsorbed in the Atop, Bridge, and 4-fold Hollow Sites in the Different Arrangements Indicated.[a]

	overlayer A	overlayer B	overlayer C			
layer	4-fold hollow	4-fold hollow	3-fold hollow	4-fold hollow	bridge	atop
Fe1	**−0.15**	**−0.47**	**0.04/0.05**	**0.05/0.06**	**−0.41**	**−0.12**
	0.26	0.39	−0.03	0.35	0.43	0.44
			0.35			
Fe2	0.07	0.11	0.03	0.06	0.09	0.10
	0.09	0.12	0.08	0.20	0.10	0.12
			0.19			
Fe3	0.09	0.10	0.10	0.12	0.12	0.11
		0.14	0.11		0.13	0.12
Fe4	0.09	0.12	0.12	0.12	0.12	0.12
	0.13	0.14	0.13	0.13	0.13	
Fe5	0.34	0.34	0.34	0.34	0.34	0.34
	0.36	0.35			0.35	

[a] Atoms directly bonded to the adsorbed S are shown in bold type. The values for atoms which are symmetrically equivalent are shown only once.

In particular, S is found to reduce the μ_B enhancement of the surface layer Fe atoms most closely bonded to the adsorbed S, as compared to the clean surface. In some cases this even leads to a negative $\Delta\mu_B$ value, as the magnetic moment value is smaller than the bulk value. As mentioned above, this quenching of the magnetic moment enhancement indicates the occurrence of spin pairing after S adsorption. The μ_B enhancement values of the 2nd most closely bonded Fe atoms were also found to change after S adsorption, indicating that the S interacts with these atoms as well. The values were not altered as much as they were for the most closely bonded Fe atoms, as the interaction is weaker.

3.4. Density of States. The local partial density of states (DOS) are presented in Figure 3 for the two structures calculated to be minima, the 4-fold hollow overlayer A and the 3-fold hollow overlayer C arrangements. They are shown for the adsorbed S atom as well as the Fe atoms that are directly bonded to the adsorbed S atom. The corresponding clean surface Fe DOS are presented for comparison.

For the 4-fold hollow overlayer A arrangement, there are some minor changes to the Fe d-orbital DOS after S adsorption, with all showing a shift to higher energy and an increase in states at ∼5 eV below E_F. The increase is greater for the Fe $d_{x^2-y^2}$, d_{xy}, d_{yz}, and d_{xz} orbitals, with the Fe d_{z^2} orbital showing a smaller increase, but indicating the interaction is rather delocalized. The energy of the new states is consistent with ultraviolet photoemission spectroscopy data which show a S-induced peak at 4.6 eV below E_F.[30]

For the 3-fold hollow overlayer C arrangement, there is also an increase in Fe d-orbital states at ∼5 eV below E_F after S adsorption. However, the increase is primarily for the Fe d_{xy}

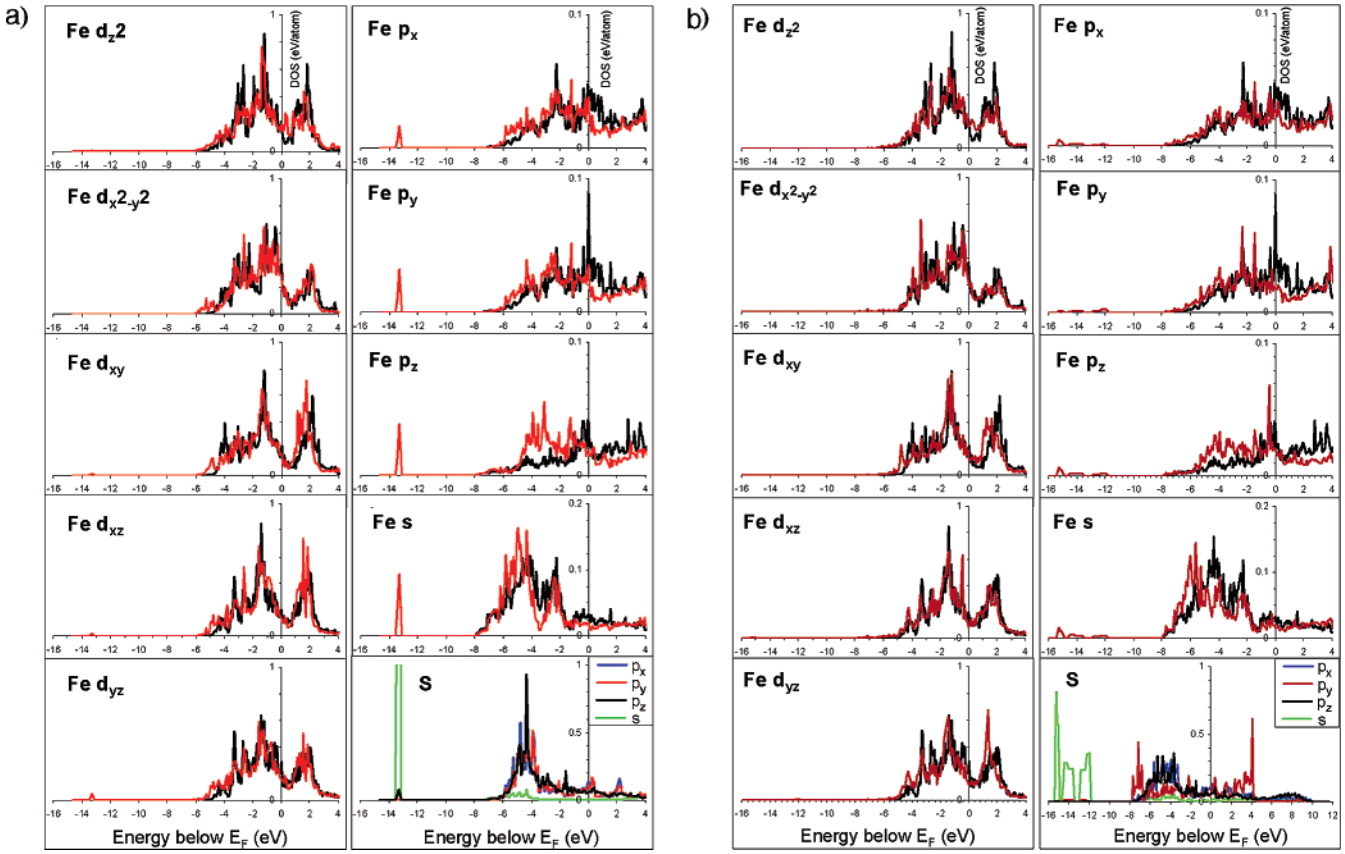

Figure 3. Orbital resolved local density of states (LDOS) for the adsorbed S atom (color as indicated) as well as the Fe atom (red) directly bonded to the S adsorbed in a (a) 4-fold hollow site at 1/3 ML coverage in the overlayer A arrangement (b) and 3-fold hollow site at 1/3 ML coverage in the overlayer C arrangement. The LDOS for the clean Fe(110) surface atoms (black) are also shown.

orbitals, followed by the Fe d_{yz} and d_{xz} orbitals which show respectively smaller changes in states. The d_{z^2} and $d_{x^2-y^2}$ DOS only show minor increases in states at this energy. Hence, unlike the 4-fold hollow overlayer A arrangement, the interaction of the adsorbed S in this site is more localized, being stronger with the d_{xy} and d_{yz} orbitals.

For both overlayer arrangements, the S also interacts with the Fe $p_{x,y,z}$ and s orbitals. Similar to the d-orbital DOS, the changes to the Fe p-orbitals DOS are smaller for the 3-fold overlayer C arrangement, indicating a weaker interaction. There is also an additional peak at −13.5 eV which is largest in the Fe s DOS.

For both arrangements, the DOS for the adsorbed S atom after adsorption on the surface are considerably different. For the 4-fold overlayer A arrangement, the DOS of the S s-orbital are located at ∼−13.5 eV below E_F and are quite narrow. The S p-orbital DOS are also relatively narrow, extending to −6 eV below E_F and are all of similar intensity. In contrast, the DOS for the 3-fold hollow overlayer C arrangement are significantly broader, with the S s-orbital DOS extending from approximately −12 to −16 eV. The S p-orbital DOS are also broader and extend down to ∼ −8 eV below E_F. This indicates that the adjacent S atoms interact with each other in this arrangement and is consistent with the close proximity of the S atoms on the surface. Such changes were also seen for the DOS of S/Fe(110) at 1 ML coverage[1] where the adjacent S−S distances were also 2.47 Å. In addition, the S p-orbital DOS are broadened more than the S p_x or p_z DOS for the 3-fold hollow site, consistent with the localized bonding with Fe orbitals along the *y*-direction.

3.5. Charge Density. The charge density plots, taken along the shortest S−S direction are presented in Figure 4 for the 3-fold hollow overlayer C and 4-fold hollow overlayer A arrangements.

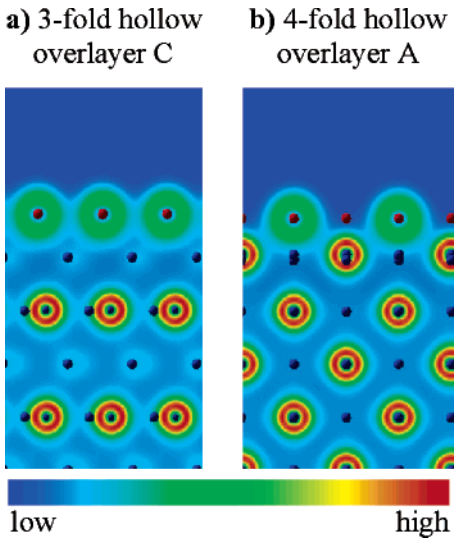

Figure 4. Charge density slices through the (a) 3-fold hollow overlayer C and (b) 4-fold hollow overlayer A arrangements. Slices are taken along the direction of the shortest S−S distance.

These plots clearly show the interaction between adjacent S atoms for the 3-fold hollow overlayer C arrangement but not for the other more stable arrangement where the S atoms sit further apart on the surface, as was suggested by the DOS and geometry of these overlayers. Hence, the interaction between adjacent S atoms for overlayer C results in the S sitting higher on the surface, leading to a less stable overlayer.

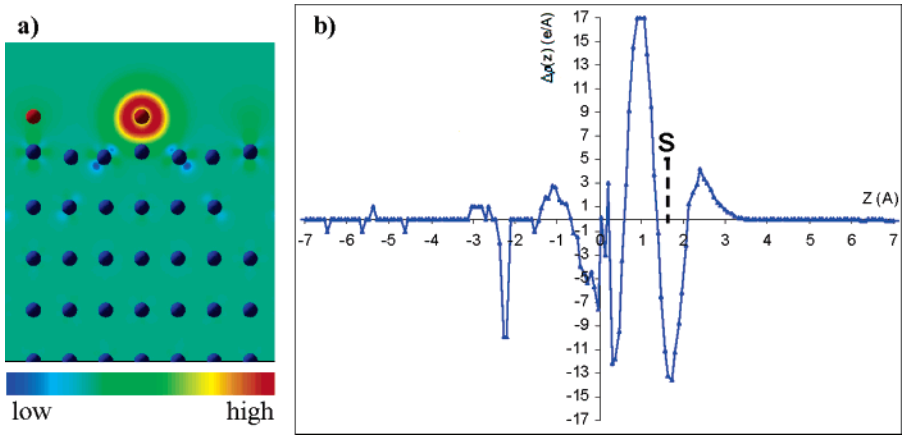

Figure 5. Charge density difference plots of S/Fe(110) in 4-fold hollow sites with S arranged as in overlayer A; (a) charge density difference slice through the shortest S−S distance; (b) planar averaged charge density change upon S adsorption. The average *z*-position of the topmost Fe layer is aligned to zero. The position of the adsorbed S atom is indicated by the dashed line.

Similar to our previous study at other S coverages,[1] the plots taken along different directions through the surface give an indication of the surface Fe atoms most strongly involved in bonding to the adsorbed S atom. For the 3-fold hollow site, the three closest Fe atoms are 2.25, 2.30, and 2.35 Å away from the S. The charge density plots indicate that the interaction with the two closest of these atoms is slightly stronger than the atom furthest away. For the 4-fold hollow site, the S interacts primarily with the two closest Fe atoms in the surface layer. There is little interaction with the next two closest atoms.

The charge density difference plot for the 4-fold hollow overlayer A arrangement is presented in Figure 5a. It was calculated by subtracting the charge density of the clean Fe(110) surface and isolated S atoms (in their positions after S adsorption and relaxation) from that of the S/Fe(110) system. This plot shows that the charge is concentrated around the S atoms, in agreement with the work function change which indicated the S behaves as an electronegative species causing a transfer of charge from the surface to the adsorbate. Some small depletion of charge can also be seen around some of the 2nd layer Fe atoms, indicating that S does interact with these atoms and explaining the change in magnetic moment enhancement values discussed earlier for these atoms after S adsorption.

To further examine how the S affects the electron density of the system after adsorption, the planar-averaged charge density difference plot (see Figure 5b), in slices perpendicular to the surface normal (*z*), defined as $\Delta\rho_{(z)}$, was calculated with the following equation:

$$\Delta\rho_{(z)} = \rho_{(z)}\mathrm{S/Fe(110)} - \rho_{(z)}\mathrm{Fe(110)} - \rho_{(z)}\mathrm{S}$$

where $\rho_{(z)}$S/Fe(110), $\rho_{(z)}$Fe(110), and $\rho_{(z)}$S are the planar averaged density along the *z*-direction (perpendicular to surface plane) of the adsorption system, the isolated clean surface and isolated S atoms, respectively, all at their relative positions in the adsorption system. The plot is aligned so that the average position of the topmost Fe layer is at zero, and the position of the adsorbed S atom is indicated by a dashed line.

The plot clearly shows that the charge density is not evenly distributed throughout the system. In particular, a large accumulation of charge is present in the region between the adsorbed S atom and the topmost Fe surface layer. The position of this accumulation, however, is closer to the S atom than to the Fe layer, which is indicative of polar covalent bonding. Such bonding was observed for S adsorbed at other coverages on the Fe(110) surface.[1] The regions of charge accumulation and depletion in the lower Fe layers are much smaller, consistent with the decreased interaction of the adsorbate with these layers that was reflected in the calculated structural and magnetic moment values.

4. Conclusion

Density functional theory calculations have been performed to distinguish between the stability and properties of the different overlayer arrangements of S on Fe(110) at 1/3 ML coverage that have been observed experimentally.

It was found that S is most stable in the overlayer arrangement formed after dissociative adsorption of H_2S on Fe(110) with S adsorbed in 4-fold hollow sites. This arrangement corresponds to a minimum on the potential energy surface. The S causes a minor-adsorbate induced reconstruction of the surface atoms that leads to an increase in the coordination of the adsorbed S and quenching of the magnetic moment of the Fe atoms most closely bound to the adsorbate. The S behaves as an electronegative surface species, causing a positive work function change and forming a polar covalent bond to the surface. The bonding is rather delocalized in this site, with the strongest interaction being with orbitals of *x*,*y* character.

No minimum energy structure was found for the overlayer arrangement formed via S segregation, indicating that the presence of subsurface S atoms may stabilize this overlayer. Again, the S caused a positive work function change and quenched the magnetic moment of the most closely bound Fe atoms.

In the alternate overlayer arrangement, S was most stable in 3-fold hollow sites, with the structure corresponding to a minimum on the potential energy surface that was less stable than the other arrangements. The reduced stability of this overlayer was attributed to the interaction of adjacent S atoms which where located closest together in this arrangement, leading to a more localized bonding, with the interaction of S with the surface being stronger with orbitals of *y*-character.

Acknowledgment. Useful discussions with Associate Professor Graeme L. Nyberg are gratefully acknowledged. Ms Nevena Todorova is acknowledged for running some of the stationary-point classification calculations. The Victorian Partnership for Advanced Computing (VPAC) and Australian Partnership for Advanced Computing (APAC) are acknowledged for provision of computer time grants.

References and Notes

(1) Spencer, M. J. S.; Snook, I. K.; Yarovsky, I. *J. Phys. Chem. B* **2005**, *109*, 9604.
(2) Kelemen, S. R.; Kaldor, A. *J. Chem. Phys.* **1981**, *75*, 1530.
(3) Oudar, J. *Bull. Soc. fr. Mineral. Cristallogr.* **1971**, *94*, 225.
(4) Berbil-Bautista, L.; Krause, S.; Hanke, T.; Bode, M.; Wiesendanger, R. *Surf. Sci.* **2005**, in review.
(5) Weissenrieder, J.; Gothelid, M.; Le Lay, G.; Karlsson, U. O. *Surf. Sci.* **2002**, *515*, 135.
(6) Taga, Y.; Isogai, A.; Nakajima, K. *Trans. Jpn Inst. Met.* **1976**, *17*, 201.
(7) Spencer, M. J. S.; Hung, A.; Snook, I.; Yarovsky, I. *Surf. Sci.* **2003**, *540*, 420.
(8) Kresse, G.; Furthmuller, J. *Phys. Rev. B* **1996**, *54*, 11169.
(9) Kresse, G.; Furthmuller, J. *Comput. Mater. Sci.* **1996**, *6*, 15.
(10) Kresse, G.; Hafner, J. *Phys. Rev. B* **1993**, *48*, 13115.
(11) Kohn, W.; Sham, L. J. *Phys. Rev.* **1965**, *140*, 1133.
(12) Perdew, J. P.; Yue, W. *Phys. Rev. B* **1992**, *45*, 13244.
(13) Vanderbilt, D. *Phys. Rev. B* **1990**, *41*, 7892.
(14) Monkhorst, H. J.; Pack, J. D. *Phys. Rev. B* **1976**, *13*, 5188.
(15) Hung, A.; Yarovsky, I.; Muscat, J.; Russo, S.; Snook, I.; Watts, R. O. *Surf. Sci.* **2002**, *501*, 261.
(16) Spencer, M. J. S.; Hung, A.; Snook, I. K.; Yarovsky, I. *Surf. Sci.* **2002**, *515*, L464.
(17) Spencer, M. J. S.; Hung, A.; Snook, I.; Yarovsky, I. *Surf. Rev. Lett.* **2003**, *10*, 169.
(18) Spencer, M. J. S.; Hung, A.; Snook, I. K.; Yarovsky, I. *Surf. Sci.* **2002**, *513*, 389.
(19) Hung, A.; Muscat, J.; Yarovsky, I.; Russo, S. P. *Surf. Sci.* **2002**, *520*, 111.
(20) Hung, A.; Muscat, J.; Yarovsky, I.; Russo, S. P. *Surf. Sci.* **2002**, *513*, 511.
(21) Muscat, J.; Hung, A.; Russo, S.; Yarovsky, I. *Phys. Rev. B* **2002**, *65*, 054107/1.
(22) Spencer, M. J. S.; Snook, I. K.; Yarovsky, I. *J. Phys. Chem. B* **2004**, *108*, 10965.
(23) Spencer, M. J. S.; Snook, I. K.; Yarovsky, I. *J. Phys. Chem. B* **2005**, *109*, 10204.
(24) Methfessel, M.; Paxton, A. T. *Phys. Rev. B* **1989**, *40*, 3616.
(25) Blochl, P. E.; Jepsen, O.; Andersen, O. K. *Phys. Rev. B* **1994**, *49*, 16223.
(26) Makov, G.; Payne, M. C. *Phys. Rev. B* **1995**, *51*, 4014.
(27) Neugebauer, J.; Scheffler, M. *Phys. Rev. B* **1992**, *46*, 16067.
(28) Shih, H. D.; Jona, F.; Jepsen, D. W.; Marcus, P. M. *Phys. Rev. Lett.* **1981**, *46*, 731.
(29) Yarovsky, I.; Spencer, M. J. S.; Snook, I. Iron surfaces and interfaces: structure and properties from Density Functional Theory. In *Progress in Surface Science*; Columbus, F., Ed.; Nova Science Publishers: Hauppauge, NY, 2005; in press.
(30) Broden, G.; Gafner, G.; Bonzel, H. P. *Appl. Phys.* **1977**, *13*, 333.